IV. RADIO ASTRONOMY*

Academic and Research Staff

Prof. A. H. Barrett	Prof. D. H. Staelin	Dr. J. W. Waters
Prof. B. F. Burke	Dr. K. F. Kunzi	J. W. Barrett
Prof. R. M. Price	Dr. G. D. Papadopoulos	D. C. Papa

Graduate Students

B. G. Anderson	C. A. Knight	P. C. Myers
K. P. Bechis	K-S. Lam	R. M. Paroski
P. C. Crane	K-Y. Lo	R. K. L. Poon
P. L. Kebabian	R. N. Martin	J. H. Spencer
V. T. Kjartansson		A. R. Whitney

RESEARCH OBJECTIVES AND SUMMARY OF RESEARCH

The program in radio astronomy comprises very long baseline interferometry, in which highly stable atomic frequency standards are used to control frequency and time to permit the operation of radio interferometry over arbitrarily long baselines; radio spectroscopy of the interstellar medium, specifically studies of interstellar molecular emission and absorption; the study of pulsars; and the use of radio astronomical techniques to study the Earth's atmosphere.

1. Aperture Synthesis

A three-element interferometer consisting of 18 ft antennas on a 1000-ft baseline is being constructed on the site of the Haystack Observatory. One antenna will be movable over approximately 500 feet with the other two fixed at a 500-ft spacing. The interferometer will be instrumented for 1.75 cm and used to study the brightness distributions of the strong radio sources.

2. Very Long Baseline Interferometry (VLBI)

The program of VLBI observations continues the study of galactic sources of H_2O spectral line emission at 1.35 cm. Successful experiments have been carried out using the Haystack radio telescope in Westford, Massachusetts, and the 22 m radio telescope of the Crimea Astrophysical Observatory, near Yalta, U.S.S.R. (Lat. 44°.4, Long. 34°).

This has led to a determination of source sizes of approximately 0.0003 second of arc, the highest angular resolution ever achieved. Only the strongest lines have been studied because of limitations on observing time. This work is continuing.

3. Microwave Spectroscopy of the Interstellar Medium

Many molecules have been detected by radio techniques in the interstellar medium, and our studies are concentrating on OH, H_2O, CH_2 (formaldehyde), and CH_3OH (methyl alchol). OH and CH_2O are widespread throughout the galaxy, whereas H_2O and

*This work was supported principally by the National Aeronautics and Space Administration (Grants NGL 22-009-016, NGR 22-009-421), and Langley Research Center Contract NAS1-10693, and the National Science Foundation (Grants GP-20769, GP-21348, and GP-14589); and in part by California Institute of Technology Contract 952568, and the Sloan Fund for Basic Research (M.I.T., Grant 241).

CH_3OH appear to be present only in limited regions of high density. Correlation studies of OH and CH_2O in selected interstellar clouds have been made.

4. Radio Astronomy Studies of the Earth's Atmosphere

The program of balloon-based atmospheric observations continues. In addition, ground-based studies of the upper atmospheric ozone, H_2O, and oxygen have been carried out to determine water-vapor content and temperature structure of the mesosphere and the stratosphere. An aircraft-borne radiometer has been tested, preliminary to the satellite-borne oxygen and water observations to be conducted in the Nimbus series.

A. H. Barrett, B. F. Burke

A. OBSERVATIONS OF RECOMBINATION LINES AT Ku-BAND

Measurements of excited hydrogen 73α recombination lines in the galactic HII regions of Orion A, W3, W49, and W51 have been performed at 16.56 GHz. The purpose of these short-wavelength observations was to help distinguish between local thermodynamic equilibrium (LTE) and non-LTE models of atomic energy level populations by Hnα line observations for $n \lesssim 80$.

The observations were made in May 1971 with the 36.5 m antenna of the Haystack Observatory. The telescopic system was calibrated toward several standard sources that were monitored periodically throughout the experiment. The half-power beamwidth at 16.6 GHz was determined to be 2.1 minutes of arc, and the overall aperture efficiency was measured as 20 ±5%. The radiometer, which is an uncooled degenerate parametric amplifier followed by a mixer preamplifier, was designed and constructed by members of the Research Laboratory of Electronics, M.I.T. The noise temperature of the parametric amplifier was 120°K, the gain 18 dB, and the bandwidth approximately 60 MHz. The measured single-sideband system temperature was ~450°K.

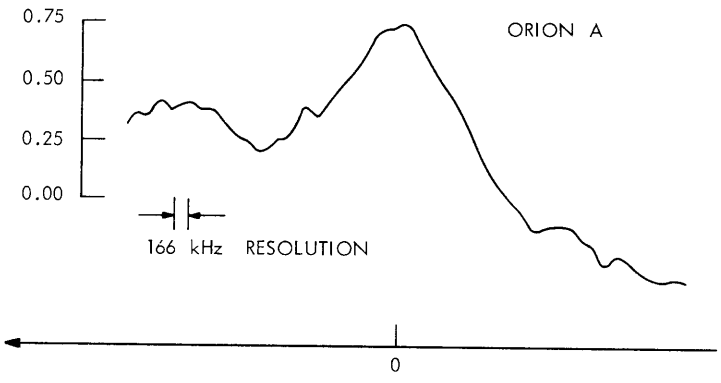

Fig. IV-1. Line profile for Orion A.

The spectrometer was a 100-channel 1-bit digital autocorrelator. The spectral resolution was 500 kHz (9.05 km s^{-1}) for a predetection bandwidth of 20 MHz. Source spectra were obtained by using the technique of total-power observing, in which unswitched observations of 5-min duration were made sequentially off and on the position of maximum nebular intensity.

Table IV-1. Summary of observed and derived quantities.

Source	α (1950.0)	δ (1950.0)	T_L (°K)	V_{LSR} (km s^{-1})	$\Delta\nu_L$ (km s^{-1})[a]
Orion A[b]	$05^h\ 32^m\ 51^s$	-05°25'00"	0.72 ± 0.04	-0.5 ± 0.7	26.6 ± 2
W3A	02 21 55	61 51 59	0.22 ± 0.04	-40.2 ± 2	22.4 ± 5
W49A	19 07 54	09 01 01	0.22 ± 0.08	+2.2 ± 8	27.1 ± 10
W51	19 21 23	14 24 29	0.33 ± 0.04	+57.0 ± 2	26.8 ± 4

$\Delta\nu_L$ (kHz)[a]	T_c (°K)	T_e^* (°K)
1475 ± 110	5.6 ± 0.5[c]	$10700\ ^{+1800}_{-1400}$
1250 ± 280	2.0[d]	$13500\ ^{+4600}_{-4000}$
1500 ± 550	1.8[d]	$11000\ ^{+6300}_{-5500}$
1480 ± 220	3.0 ± 0.4[c]	$12000\ ^{+3000}_{-2600}$

Notes: All errors are 3σ.
a = Corrected for instrumental broadening.
b = 166 kHz (3.0 km s^{-1}) spectral resolution in observations.
c = A measured value.
d = An adopted value; estimated error ~15%.

The measured line profile of Orion A for a 180-min integration is shown in Fig. IV-1. The parameters for each source were obtained from the spectral lines by means of a least-squares Gaussian analysis. In Table IV-1 the observational coordinates, the antenna temperature in the spectral line, the radial velocity relative to the local standard of rest (LSR), and the spectral fullwidth in frequency and velocity units are listed for each nebula. The continuum antenna temperature, T_c, was obtained concurrently with the line measurements for Orion A and W51. The LTE electron temperature, T_e^*, is calculated from Eq. 1, which is given by Mezger and Höglund.[1] In arriving at this expression they assumed that the atomic emitters are electronically populated according to local thermodynamic equilibrium and that the plasma is optically thin.

$$T_e^* = \left[2.28 \times 10^4 \, \frac{\nu^{2.1} T_c}{\Delta\nu_L T_L} \right]^{1/1.15} . \qquad (1)$$

Here T_c and T_L are the continuum and spectral-line antenna temperatures in °K, ν is the frequency of observation in GHz, and $\Delta\nu_L$ is the spectral fullwidth at half power in kHz. The constant includes the proper factor for the ratio of the assumed and exact expressions for free-free absorption[2] and a correction for a number density ratio of singly ionized helium-to-hydrogen atoms of 0.08.

The electron temperatures determined for each nebula by means of Eq. 1 are distinctly higher than those found previously at lower frequencies. These deviations at the high frequencies have been predicted by non-LTE models developed by Hjellming and Davies[3] and by Goldberg and Cesarsky.[4] Each shows that a convenient test of the non-LTE model entails observation of recombination lines for principal quantum numbers $n \lesssim 80$. At these high frequencies the non-LTE model predicts a true electron temperature lower than that obtained from the optically thin LTE solution. Our calculated values of T_e^* for all nebulae are in agreement with the general high-frequency predictions of the non-LTE theory.

A more detailed account of our observations will appear in a paper submitted for publication to Astrophysical Letters.

G. D. Papadopoulos, K. Y. Lo, P. Rosenkranz,
E. J. Chaisson

[E. J. Chaisson is at the Harvard College Observatory.]

References

1. P. G. Mezger and B. Höglund, Astrophys. J. 147, 490 (1967).
2. P. G. Mezger and A. P. Henderson, Astrophys. J. 147, 471 (1967).
3. R. M. Hjellming and R. D. Davies, Astron. Astrophys. 5, 53 (1970).
4. L. Goldberg and D. A. Cesarsky, Astrophys. Letters 6, 93 (1970).

B. RADIOMETER SYSTEM FOR GROUND-BASED MEASUREMENT OF UPPER ATMOSPHERIC TEMPERATURES

A 53-GHz radiometer, 24-channel IF filter bank, and data recording system are being constructed for studies of atmospheric microwave emission from high angular momentum spin-rotation transitions of molecular oxygen. Ground-based measurements of this emission provide data on atmospheric temperature variations up to altitudes of approximately 60 km with approximately 16-km resolution.[1] These data are useful for understanding the dynamics of the Earth's upper atmosphere. Results of

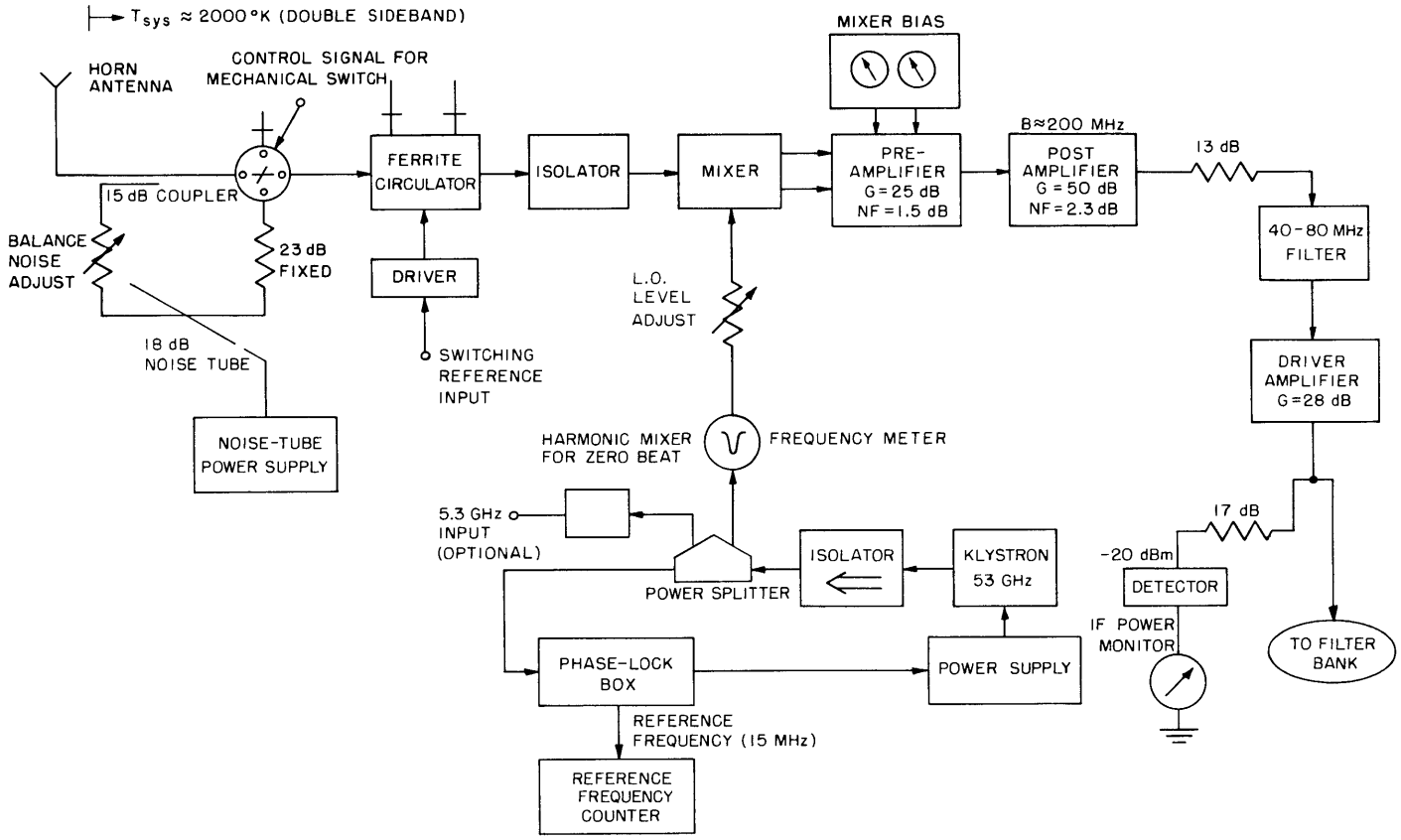

Fig. IV-2. Radiometer.

ground-based experiments will also be useful for designing appropriate experiments to be made from satellite platforms.

A block diagram of the radiometer is shown in Fig. IV-2. A bench model was built and tested and the components are now being packaged in a portable, temperature-controlled box. The mixer was obtained from R. W. Chick of Group 63 of Lincoln Laboratory, M. I. T., and a low-noise preamplifier was constructed at the Research Laboratory of Electronics, M.I.T., by D. H. Steinbrecher and V. T. Kjartansson. The measured double-sideband noise figure of the mixer-preamplifier combination at 53 GHz RF and 60 MHz IF is approximately 6.5 dB. Additional losses of 2.5 dB in the microwave circuitry in front of the mixer give an overall single-sideband receiver noise temperature of 4000°K, as compared with 20,000°K for the receiver that we used in previous measurements of emission from the 27_{-} O_2 line at 53 GHz. For 1-hour integration time and 1-MHz frequency resolution with a switched radiometer, the theoretical rms noise of the present system is 0.13°K. From sea level the amplitude of the strongest oxygen emission line is 10°K, so that the present system should be able to measure this line with an rms accuracy of 1.3%. A 1% change in the strength of the oxygen emission corresponds to a 0.2% change in atmospheric temperature. This suggests that theoretically the present system can monitor upper-atmospheric temperature changes with an rms accuracy of ~0.25% or ~0.6°K over a time period of 1 hour. The actual performance will be partially limited by calibration errors.

Frequency stabilization of the local oscillator in a single phase-lock loop is accomplished by using a commercial microwave oscillator frequency stabilizer that is specified to operate only at frequencies below 40 GHz, but which we used to stabilize directly the 53-GHz klystron in the radiometer.

The filter bank includes one total-power channel and 23 filtered channels (Fig. IV-3). The center frequency of the filter bank was chosen at 60 MHz because this is a convenient frequency range for the construction of filters with the bandwidths required for the ground-based experiment. The center frequencies and bandwidth of the filters superimposed upon the oxygen line shape are shown in Fig. IV-4. A total of 24 channels was chosen because multiplex units for the analog-to-digital converter in the data-processing system are available with the number of inputs in multiples of eight, and because approximately 24 channels are needed to study the line shape. All of the components of the filter bank except the detector and dc amplifier circuit were purchased. The detectors and dc amplifiers were built at the Research Laboratory of Electronics, M. I. T., and tested for linearity and sensitivity.

The detected output of each channel is synchronously detected and averaged by a small commercial computer and recorded on magnetic tape. The computer also controls the mechanical waveguide switch in the radiometer for automatically performing calibrations, and provides calibrated displays of spectra on a teletype printer. The

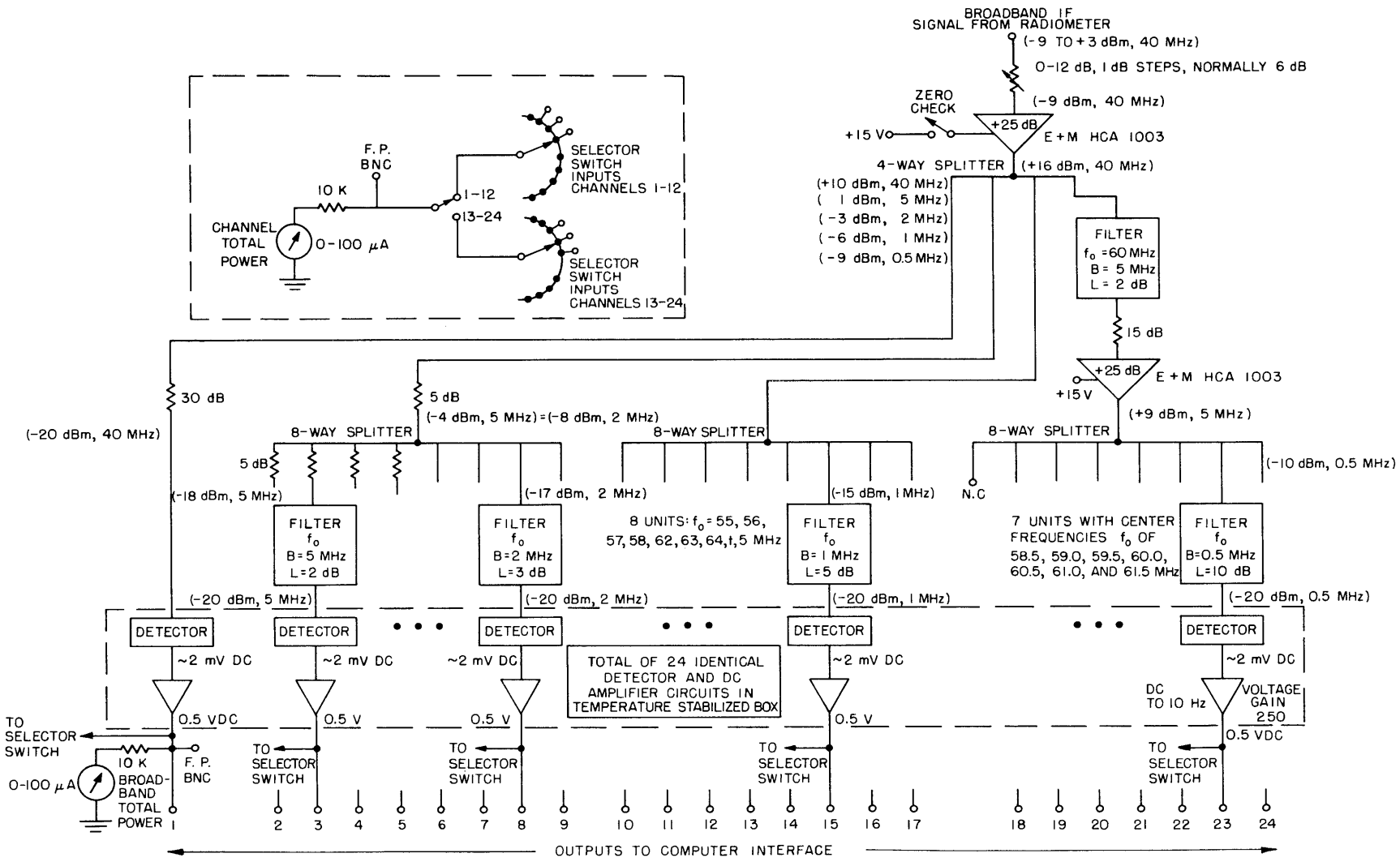

Fig. IV-3. Filter bank. Power levels at various points are in parenthesis.

hardware design of the data-recording and computer system is complete, and all components have been purchased.

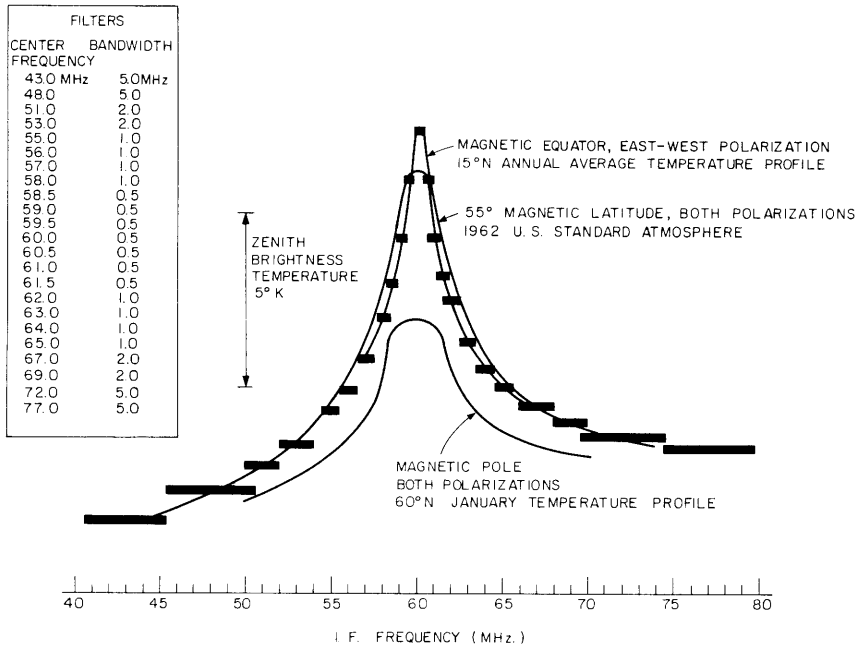

Fig. IV-4. Filter positions, bandwidths, and computed zenith emission from 27_ O_2 line.

The primary purpose of this multichannel radiometer is for ground-based studies of temperature in the upper atmosphere, but the filter bank and data-recording system constructed for it provide very versatile instruments for atmospheric and radio astronomical studies of spectral line emission. It offers an advantage over our previous spectral line receiver[2] because all essential data processing can be accomplished by the instrument itself, without recourse to external computation facilities.

J. W. Waters, J. W. Barrett, D. C. Papa,
R. M. Paroskie, D. H. Staelin

References

1. J. W. Waters, "Ground-Based Passive Microwave Sensing of Temperatures in the Stratosphere and Lower Mesosphere," paper presented at Seventh International Symposium on Remote Sensing of Environment, University of Michigan, May 17-21, 1971.
2. L. P. A. Henckels, "A Digital Output Unit for a Multichannel Radiometer," S. M. Thesis, Department of Electrical Engineering, M. I. T., June 1968.

C. CONTINUUM RADIO STRUCTURE OF THE GALACTIC DISK

From the observed brightness distribution along the galactic plane we can estimate the distribution of the emission regions in the plane and perhaps say something about the

energy sources for the observed continuum radio emission. The brightness distribution directly along b = 0° includes a contribution from discrete sources (for example, HII regions) which may not play a large role in the large-scale structure of the disk continuum radio emission at meter wavelengths. For this reason, in the present study we used the emission from a strip of ±6° of galactic latitude along the galactic equator. The solid line in Fig. IV-5 shows the resulting average brightness temperature vs galactic longitude distribution. This curve was obtained by J. Elias (at the time an undergraduate student at M. I. T.) using numerical integration over the 12° latitude strip for each degree of galactic longitude. The data were obtained from the 408-MHz surveys of Kommesaroff,[1] Large, Mathewson, and Haslam,[2] and Seeger, Westerhout, Conway, and Hoekema,[3] with their baselines normalized to the level determined by Price.[4]

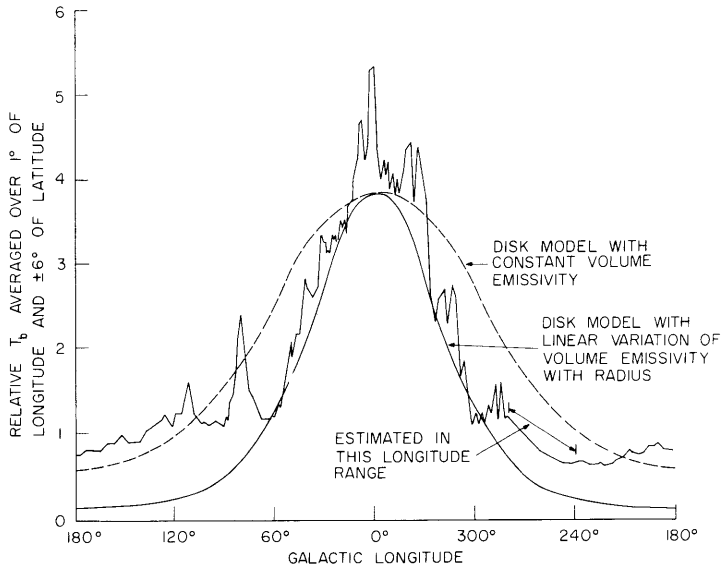

Fig. IV-5. Relative brightness temperatures along the galactic plane at 408 MHz averaged over 1° of longitude and ±6° of latitude at each degree of longitude.

The striking feature of the distribution shown in Fig. IV-5 is the sharp peaking toward the galactic center, with only a gentle falloff in intensity at longitudes greater than 60° from the center. Another prominent characteristic is the number of sharp, and often narrow, features of higher intensity. These represent discrete sources and clusters of discrete sources, for example, Cygnus X region, and the galactic center region. Figure IV-5 shows two simple models for radio emission within the disk: the dashed line illustrates a disk of radius 1.4 R_o with constant volume emissivity; the dotted line represents a model with a volume emissivity that drops off linearly with distance

from the galactic center until it reaches zero at 1.4 R_o.

The model with constant volume emissivity agrees with the high brightness temperatures observed in the anticenter region, but it is much broader in longitude than the observed distribution. On the other hand, the model with the linear falloff in volume emissivity with increasing radius is peaked toward the galactic center, but provides much less brightness temperature than is actually observed in the regions at greater than 60° from the center.

There are two other possibilities. The bulk of the radiation observed within 60° of the galactic center could arise in a disk of approximately R_o radius. This seems highly unlikely, and still leaves the emission in the anticenter region to be accounted for. The other alternative is that a large proportion of the emission is in the large-scale spiral features of the galactic plane. This was originally proposed on the basis of more limited data by Mills.[5] Recently, this distribution of continuum radiation has been strikingly shown in the external galaxy M51 by Mathewson, van der Kruit, and Brouw.[6] In M51 the spiral features give 1.5 times as much flux density as the "base" disk component. A similar situation may well exist in our own galaxy. A model of the expected brightness distribution is being prepared on the basis of the density wave model and observed neutral-hydrogen structure.

R. M. Price

References

1. M. M. Komesaroff, Australian J. Phys. 19, 75 (1965).
2. M. I. Large, D. S. Mathewson, and C. G. T. Haslam, M. N. Roy. Aston. Soc. 123, 113 (1961).
3. C. L. Seeger, G. Westerhout, R. G. Conway, and T. Hoekema, Bull. Astron. Inst. Neth. 18, 11 (1965).
4. R. M. Price, Australian J. Phys. 23, 227 (1970).
5. B. Y. Mills, in R. N. Bracewell (Ed.), Proc. Paris Symposium on Radio Astronomy, Stanford University Press, Stanford, California, 1959, p. 431.
6. D. S. Mathewson, P. C. van der Kruit, and W. N. Brouw (to appear in Astronomy and Astrophysics).

D. ABSOLUTE RADIO BRIGHTNESS TEMPERATURES IN THE SOUTHERN SKY

The analysis of observations of the Southern Sky at 408 MHz using the 210 ft antenna of the CSIRO in Australia has been completed. The result is a grid of absolute brightness temperature reference points with spacing of 15° in both galactic latitude (for $b \geq 30°$) and longitude covering most of the Southern Sky. These reference points are useful (a) for providing a framework for calibrating the high-resolution observations now being

Table IV-2. Average brightness temperature at 408 MHz in 5 × 5° region centered on given coordinates.

Galactic Latitude	-90°	-75°	-60°	-45°	-30°	+30°	+45°	+60°
0	21.0	20.0	21.0	24.4	38.9	36.4	26.5	30.8
15			16.7	25.3	28.1		37.5	
30		21.4	19.7	25.6	27.6	59.3	55.9	
45			20.3		27.8	38.6		
60		21.7	23.8		20.5			
75		22.8	22.9		26.2			
90		24.5	20.0					
105			18.7					
120		23.8	20.7					
135		28.3	21.9					
150		25.3	23.9					
165			22.2		28.5			
180		22.1	18.4	20.8	21.3			
195			18.5		17.9			
210			16.4	16.0				
225			16.1	13.8	12.5			
240			14.8	12.3	14.2			
255			14.1		19.0			
270		17.4	16.9	16.6	15.1	18.3		
285			16.0	15.7	18.0	20.3	16.9	28.8
300			14.8		20.8	28.9	23.0	30.0
315			15.4		28.3	38.5	22.0	27.6
330			18.5	23.8	28.5	33.0	24.5	20.5
345		19.4	18.6	24.1	34.6	34.0	27.5	

Note: Units, °K above absolute zero level.

carried out at 408 MHz by the University of Sydney group using the Mills Cross radio telescope, (b) as a study of the differential spectrum using the results of Yates[1] and of Landecker and Wielebinski,[2] and (c) as an investigation of the large-scale structure of the high-latitude continuum emission in our galaxy.

The observations were taken at nearly constant zenith angle and compared directly with the temperature of the south celestial pole (at the same zenith angle) to avoid calibration errors. Repeatability and analysis of the drift characteristics of the receiver indicate that the rms error in brightness temperature of any point with respect to the

south celestial pole should be less than 1°K. As the brightness temperature of the south celestial pole is known[3] with an rms error of 2.0°K, this gives a total rms error of approximately 2.2°K for each point. An additional error resulting from calibration of the brightness temperature scale would, at most, contribute another 10% of the temperature difference between the region and the south celestial pole (22.5°K).

These data are being compared with those of Landecker and Wielebinski[2] to obtain spectral information and to investigate the large-scale structure of our galaxy.

R. M. Price

References

1. K. W. Yates, Australian J. Phys. 21, 167 (1968).
2. T. L. Landecker and R. Wielebinski, Australian J. Phys., Astrophysical Supplement 16, 1970.
3. R. M. Price, Astron. J. 75, 144 (1970).

E. STELLAR INTERFEROMETER

1. Duplicating Filters

Duplicating filters, as we now know them,[1,2] all have a lowpass frequency response. Figure IV-6 illustrates a bandpass filter constructed from duplicating filters of the kind shown in Quarterly Progress Report No. 101.[1] One or more of the coefficients A_j are negative, and the bandpass frequency response is obtained as the difference between two lowpass frequency responses.

This method only works when all of the lowpass filters have the same phase response: since the impulse responses of the lowpass filters are symmetric, this is equivalent to

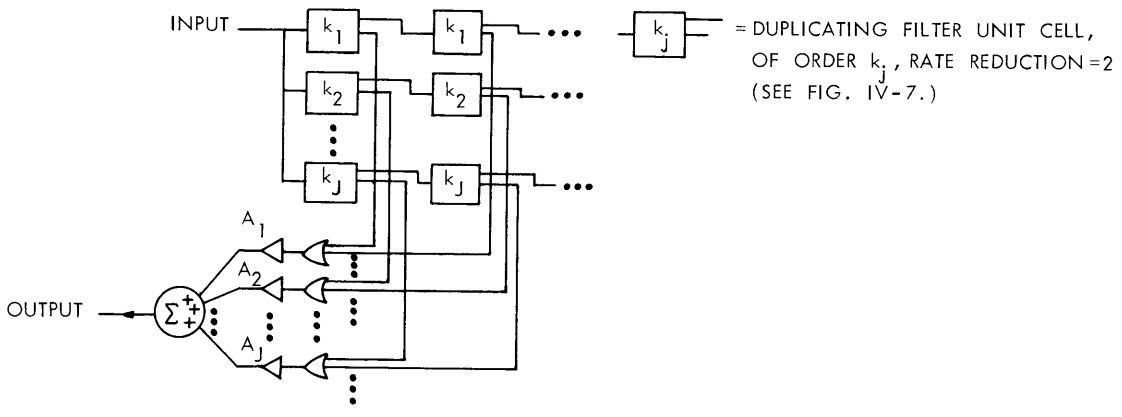

Fig. IV-6. Realization of a bandpass filter.

requiring that the centers of symmetry of the impulse responses of all of the lowpass filters occur at the same time. Note that, since they do not have symmetric impulse responses, the duplicating filters described[2] in Quarterly Progress Report No. 103, cannot, in general, be used to obtain this kind of bandpass filter.

The center of symmetry of the impulse response of an odd-order duplicating filter is located at an odd multiple of half the input period, and for an even-order filter it is located at an even multiple of half the input period. If both odd- and even-order duplicating filters are to be used to obtain a bandpass frequency response, the input to all of the odd-order filters must be delayed by ±half the input period with respect to the input to the even-order filters. This is possible by doubling the sampling rate, delaying the signal to the odd-order filters by a full cycle, and then filtering the inputs to both odd and even filters with an order 1 duplicating filter, that is, a single boxcar integrator followed by a sampler to reduce the input rate to the filters to its original value. In many practical problems, however, a better solution would be to make the duplicating filters either all odd or all even.

To shift the center of symmetry of the impulse response of one of the lower order filters to coincide with that of the highest order filter, the appropriate delay is added to the input of each of the unit cells in the lower order filter.

This method of obtaining a bandpass filter inherently requires the use of high-order duplicating filters, especially if they are all odd or all even. Therefore the unit cells must be designed to truncate the output of each stage, to prevent the word length from becoming too large. This truncation will add noise to the output of each stage, and the truncation level must be selected to keep this noise less than the quantization noise inherent in the limited number of bits in the input. An approximate analysis shows that for a single duplicating filter of S stages, the word length should be L+S/2+2, where L is the number of bits in the input signal. In a bandpass filter, the noise outputs from each of the lowpass filters are independent, and the total noise level is therefore increased by $\left(\sum_j A_j^2\right)^{1/2}$. The quantization noise input is the same to all of the filters, and the quantization noise level is reduced by the transmission loss of the bandpass filter. These two factors determine how much the word length of the bandpass filter must be increased over that required for the lowpass filters from which it is constructed.

Because the output of a duplicating filter is bursts at a submultiple, ordinarily 2, of the input rate, a single set of coefficients and summing junction can process all outputs from an arbitrarily long filter chain. No two output bursts will coincide if the output from each stage to the coefficients and summing junction is delayed by one period of the input to that stage, without delaying the output to the next stage.

Figure IV-7 shows a unit cell, similar to that shown in a previous report,[3] modified to delay the input, delay the output to the coefficients and summing

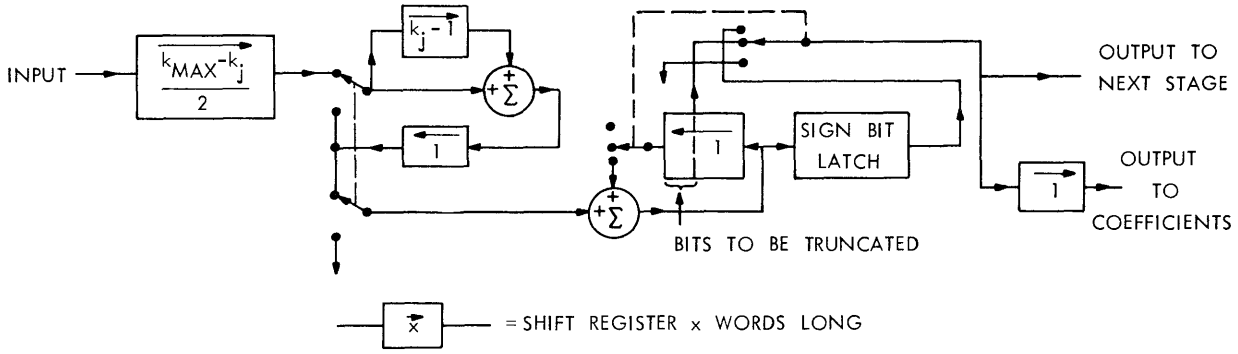

Fig. IV-7. Modified unit cell.

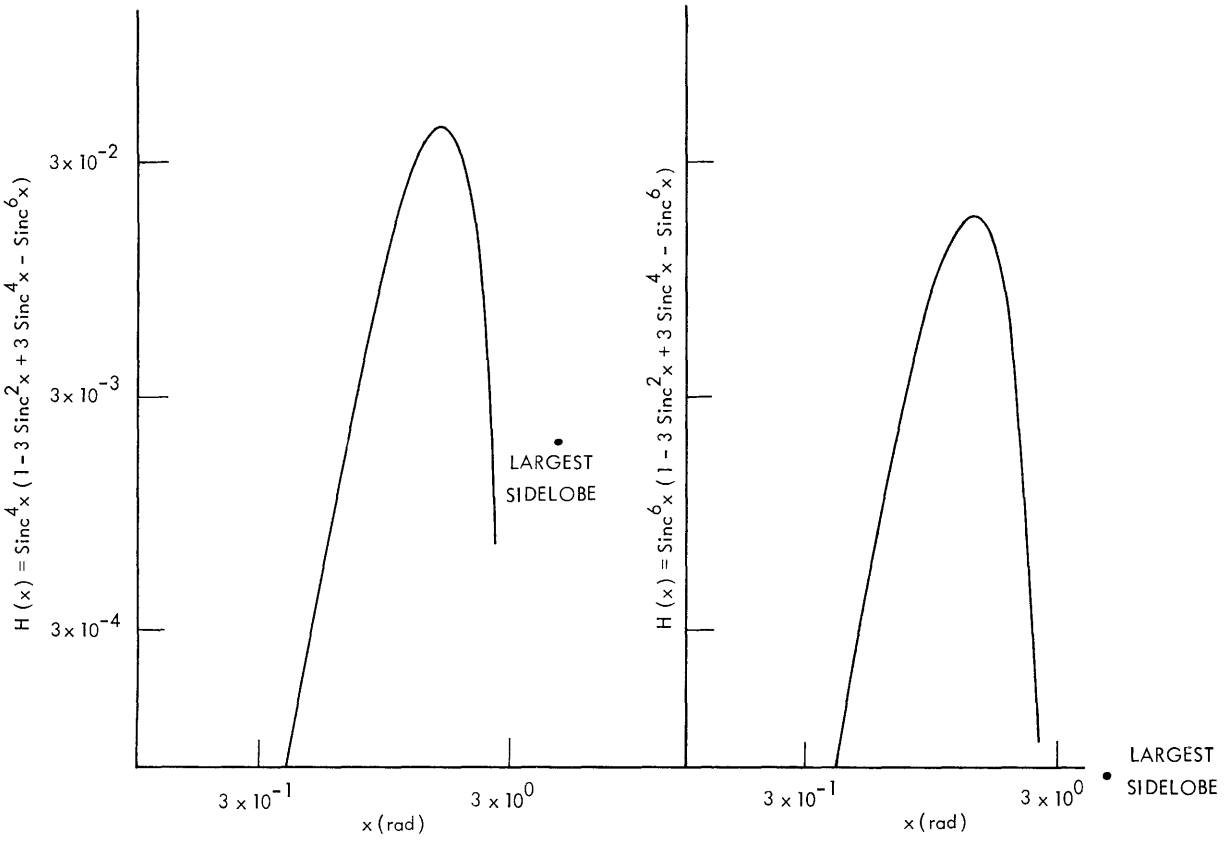

Fig. IV-8. Typical bandpass frequency response.

junction, and truncate the output, as explained above.

Figure IV-8 shows the frequency response of two typical bandpass filters. In general, the frequency response of this kind of bandpass filter is

$$H(f) = \sum_{j=1}^{J} A_j \left(\frac{\sin 2^S \pi f}{2^S \sin \pi f} \right)^{k_j}.$$

When S is not small,

$$H(f) \cong \sum_{j=1}^{J} A_j \left(\frac{\sin 2^S \pi f}{2^S \pi f} \right)^{k_j} = \left(\frac{\sin 2^S \pi f}{2^S \pi f} \right)^{k_{min}} \sum_{j=1}^{J} A_j \left(\frac{\sin 2^S \pi f}{2^S \pi f} \right)^{k_j - k_{min}}$$

for values of f, where H(f) has a significant value.

The filters in Fig. IV-8 were obtained by expanding $\left(\frac{\sin 2^S \pi f}{2^S \pi f} \right)^{k_j - k_{min}}$ as a power series and solving for the coefficients to make the terms of order $(f^2)^0$ through $(f^2)^{J-1}$ vanish.

The advantage of this kind of bandpass filter over conventional digital filters lies in its simple structure. For example, a 12^{th}-order unit cell with 48-bit words would require about the same chip area as a 1000-bit shift register. Since the coefficients are small integers, and can be realized by repeated addition, the entire filter can be built without multipliers. The package count per stage would be small, slightly over 4 in the case of the filters in Fig. IV-8.

P. L. Kebabian

References

1. P. L. Kebabian, Quarterly Progress Report No. 101, Research Laboratory of Electronics, M. I. T., April 15, 1971, pp. 1-11, see Fig. I-8.
2. P. L. Kebabian, Quarterly Progress Report No. 103, Research Laboratory of Electronics, M. I. T., October 15, 1971, pp. 20-34.
3. P. L. Kebabian, Quarterly Progress Report No. 101, op. cit., see Fig. I-10.